

REC'D MAR 27 1947

~~RESTRICTED~~  
~~CLASSIFICATION CANCELLED~~

*The Reynolds*  
PM No. 17027

**PERMANENT FILE COPY**

~~CLASSIFICATION CANCELLED~~

*J.W. Paulson*  
*12/14/53*  
**NACA**  
*OES*  
*NACA change #*  
*2109*  
*Status*

Restriction/Classification Cancelled

# RESEARCH MEMORANDUM

for the

Air Materiel Command, Army Air Forces

PRELIMINARY EVALUATION OF THE LOW-SPEED STABILITY AND CONTROL  
CHARACTERISTICS OF THE MCDONNELL XP-85 AIRPLANE FROM  
TESTS OF AN UNBALLASTED  $\frac{1}{5}$ -SCALE MODEL  
IN THE LANGLEY FREE-FLIGHT TUNNEL

By

John W. Paulson and Joseph L. Johnson

Langley Memorial Aeronautical Laboratory  
Langley Field, Va.

Restriction/Classification  
Cancelled

Restriction/Classification  
Cancelled

Sta  
US  
re  
ve  
to  
the  
Co  
ch  
the  
by

**NATIONAL ADVISORY COMMITTEE  
FOR AERONAUTICS** **FILE COPY**

WASHINGTON

To be returned to  
the files of the National  
Advisory Committee

MAR 19 1947

for Aeronautics  
Washington, D. C.

~~RESTRICTED~~  
~~CLASSIFICATION CANCELLED~~



UNCLASSIFIED

NATIONAL ADVISORY COMMITTEE FOR AERONAUTICS

RESEARCH MEMORANDUM

for the

Air Materiel Command, Army Air Forces

PRELIMINARY EVALUATION OF THE LOW-SPEED STABILITY AND CONTROL

CHARACTERISTICS OF THE MCDONNELL XP-85 AIRPLANE FROM

TESTS OF AN UNBALLASTED  $\frac{1}{5}$ -SCALE MODEL.

IN THE LANGLEY FREE-FLIGHT TUNNEL

By John W. Paulson and Joseph L. Johnson

## SUMMARY

At the request of the Air Materiel Command, Army Air Forces an investigation of the low-speed, power-off stability and control characteristics of the McDonnell XP-85 airplane is being conducted in the Langley free-flight tunnel. The XP-85 airplane is a jet propelled, parasite fighter with  $34^\circ$  sweepback at the wing quarter chord. It was designed to be carried in a bomb bay of the B-36 airplane. The first portion of the investigation consists of a preliminary evaluation of the stability and control characteristics of the airplane from force and flight tests of an unballasted  $\frac{1}{5}$ -scale model. The second portion of the investigation consists of tests of a properly ballasted  $\frac{1}{10}$ -scale model which will include a study of the stability of the XP-85 when attached to the trapeze for retraction into the B-36 bomb bay. The results of the preliminary tests with the  $\frac{1}{5}$ -scale model are presented herein. This portion of the investigation included tests of the model with various center fin arrangements. Both the design nose flap and a stall control vane were investigated.

The results of the investigation showed that the original configuration was longitudinally stable up to  $C_L = 0.6$ . At higher lift coefficients, the model showed evidence of an unstable nosing-up tendency accompanied by a violent roll-off. The use of a stall control vane to provide a stable pitching-moment curve gave good

longitudinal stability characteristics in flight over the lift coefficient range and eliminated the violent roll-off. The lateral stability and control characteristics were considered to be generally satisfactory for all conditions tested and the rolling and yawing motions were well damped.

## INTRODUCTION

An investigation of the low-speed, power-off stability and control characteristics of the McDonnell XP-85 airplane is being conducted in the Langley free-flight tunnel at the request of the Air Materiel Command, Army Air Forces. The first portion of the investigation consists of a preliminary evaluation of the stability and control characteristics from tests of a  $\frac{1}{5}$ -scale model. This relatively large scale model was used in the first tests to obtain more reliable aerodynamic data and to permit easier flight testing. Since the large size of this model made it impossible to duplicate the scaled-down wing loading, no ballasting of the model was done except that required for getting the desired center-of-gravity location. In the second portion of the investigation a  $\frac{1}{10}$ -scale model with the correct scaled-down wing loading and moments of inertia will be flown to ascertain the effects of the increased mass on stability and control characteristics. This model will also be used to study the stability of the XP-85 when attached to the trapeze for retraction into the B-36 bomb bay. The results of the tests of the  $\frac{1}{5}$ -scale model are presented herein.

The XP-85 is a jet propelled, parasite fighter designed to be carried in the forward bomb bay of the B-36. The wing has an angle of sweepback of  $34^\circ$  at the quarter chord, an aspect ratio of 4.4 and a taper ratio of 0.33. In the combat area when the need for fighter escort arises, the XP-85 is lowered from the B-36 on a trapeze arrangement and released. When further fighter protection is not required the XP-85 returns to the mother ship and is secured to the trapeze. The wings are then folded upward and the XP-85 is drawn up into the bomb bay.

The present investigation included force and flight tests of the  $\frac{1}{5}$ -scale model without power with various center fin arrangements. The model was also tested with the design nose flap and with a stall control vane.

The term "original configuration" as used in this report will refer to the model with  $-4^\circ$  wing dihedral, five tail units including the design center fin and without nose flap or stall control vane.

## SYMBOLS

S	wing area, square feet
$\bar{c}$	mean aerodynamic chord, feet
b	wing span, feet
q	dynamic pressure, pounds per square foot
$\rho$	air density, slugs per cubic foot
m	mass density, slugs per cubic foot
$\mu$	relative density factor $\left(\frac{m}{\rho S b}\right)$
$\alpha$	angle of attack of fuselage center line, degrees
$\beta$	angle of sideslip, degrees
$\psi$	angle of yaw, degrees
$C_L$	lift coefficient $\left(\frac{\text{Lift}}{qS}\right)$
$C_D$	drag coefficient $\left(\frac{\text{Drag}}{qS}\right)$
$C_m$	pitching-moment coefficient $\left(\frac{\text{Pitching moment}}{qS\bar{c}}\right)$
$C_n$	yawing-moment coefficient $\left(\frac{\text{Yawing moment}}{qSb}\right)$
$C_l$	rolling-moment coefficient $\left(\frac{\text{Rolling moment}}{qSb}\right)$

- $C_Y$  lateral-force coefficient  $\left(\frac{\text{Lateral force}}{qS}\right)$   
 $i_t$  tail incidence, degrees  
 $\delta_e$  elevator deflection, degrees  
 $\delta_a$  aileron deflection, degrees  
 $\delta_F$  nose flap deflection, degrees  
 $C_{Y\beta}$  rate of change of lateral-force coefficient with angle  
of sideslip, per degree  $\left(\frac{\partial C_Y}{\partial \beta}\right)$   
 $C_{n\beta}$  rate of change of yawing-moment coefficient with angle  
of sideslip, per degree  $\left(\frac{\partial C_n}{\partial \beta}\right)$   
 $C_{l\beta}$  rate of change of rolling-moment coefficient with angle  
of sideslip, per degree  $\left(\frac{\partial C_l}{\partial \beta}\right)$

## Subscripts:

- U upper  
L lower  
R right  
t tail

## APPARATUS

## Wind Tunnel

The investigation was made in the Langley free-flight tunnel which is designed to test free-flying dynamic models. A complete description of the tunnel and its operation is given in reference 1.

The force tests to determine the aerodynamic characteristics of the model were made on the free-flight tunnel six component balance which is described in reference 2. This balance rotates in yaw with the model so that all forces and moments are measured with respect to the stability axes. The stability axes are a system of axes in which the Z-axis is in the plane of symmetry, perpendicular to the relative wind, and directed downward; the X-axis is in the plane of symmetry perpendicular to the Z-axis and directed forward; and the Y-axis is perpendicular to the plane of symmetry and directed to the right. A sketch showing the positive directions of the forces and moments is given in figure 1.

#### Model

The  $\frac{1}{5}$ -scale model used in the investigation was constructed at the Langley Laboratory. A three-view drawing of the model is presented in figure 2 and photographs of the model are given in figures 3, 4, and 5. Table I gives the dimensional and mass characteristics of the full-scale design and scaled-up dimensional and mass characteristics of the model. With this large model it was not possible to obtain duplication of the scaled-down weight and radii-of-gyration characteristics because the maximum airspeed of the tunnel is too low to fly the model with the scaled-down wing loading. In the tests of the  $\frac{1}{10}$ -scale model, however, the proper weight and radii-of-gyration will be represented.

The wing of the model had a modified Rhode St. Genese 35 airfoil section. The substitution of this section for that specified for the full-scale design (NACA 65-010) was in accordance with the free-flight tunnel practice of using low-scale high-lift airfoils to obtain a maximum lift coefficient in the low-scale tests more nearly equal to that of the full-scale design than is possible with the design airfoil. Because of the large amount of camber in the airfoil section the trailing edge of the wing was reflexed upward so as to give about the same basic pitching moment at zero lift as the airplane with the design airfoil, and the wing was set at  $-1^\circ$  incidence so that zero lift would be obtained at approximately the same angle of attack as for the airplane. The model had been completed before the latest design changes were received and therefore the wing is farther aft than is now specified on the full-scale design and has  $0^\circ$  washout instead of  $5^\circ$ . (See table I.)

The three different center fin configurations used on the model (fig. 2) were as follows: (1) design center fin, (2) center fin twice the area of the design fin, and (3) center fin off.

For some of the tests the design nose flap, deflected downward  $30^\circ$ , was installed on the model (see fig. 2). A stall control vane was also placed on the upper surface of the wing at half the semispan and parallel to the plane of symmetry for a few tests. (See fig. 2.)

## TESTS

### Force Tests

Force tests were made to determine the static stability characteristics of the model in its original configuration and also with the large center fin installed and with the center fin removed. A few tests were made with the design nose flap installed and with the stall control vane attached. Aileron effectiveness tests were made at  $\alpha = 9^\circ$ ,  $12^\circ$ , and  $20^\circ$ . All force tests were run at a dynamic pressure of 3.0 pounds per square foot, which corresponds to an airspeed of about 34 miles per hour at standard sea-level conditions and to a test Reynolds number of 302,000 based on the mean aerodynamic chord of 1.03 feet.

All forces and moments for the free-flight-tunnel model are referred to the stability axes originating at a center-of-gravity position of 26.7 percent of the mean aerodynamic chord and 0.05 mean aerodynamic chord above the thrust line unless otherwise specified.

### Flight Tests

Flight tests were made to determine the general flying characteristics of the model over a speed range corresponding to a range of lift coefficients from 0.48 to 0.82 at a center-of-gravity position of 22.4 percent of the mean aerodynamic chord. The model was flown over the speed range with each of the tail arrangements that was force tested. No flights were attempted with the design nose flaps installed but flight tests were made with the stall control vane installed.

## RESULTS AND DISCUSSION

Force tests. - The results of the force tests made to determine the longitudinal stability characteristics of the free-flight-tunnel model are presented in figure 6. Unpublished data from higher speed

tests of a  $\frac{1}{6}$ -scale model at UWAL (University of Washington Aeronautical Laboratory) and at Wright Field are also presented on this figure. The UWAL and Wright Field data were obtained at dynamic pressures of 50.6 and 25.58, respectively. The pitching-moments have been transferred to 26.7 percent of the mean aerodynamic chord for both sets of data.

The data of figure 6 show that the free-flight-tunnel model had less static margin than the UWAL and Wright Field results indicate. The free-flight-tunnel and Wright Field data show a reduction in static margin with increasing lift coefficient indicating the presence of an unstable nosing-up tendency at the stall. The UWAL test results, however, do not show this trend but indicate nearly constant stability up to the stall. The free-flight-tunnel data are also presented for a center-of-gravity position of 22.4 percent mean aerodynamic chord which was the center-of-gravity position used in the flight tests to increase the static margin to approximately that shown by the Wright Field data.

Results of the tests made with the design nose flap deflected downward  $30^\circ$  are presented in figure 7 along with similar data from UWAL and Wright Field. These results indicate that the nose flap was ineffective on the free-flight tunnel model while the corresponding data from UWAL and Wright Field showed that the flap resulted in an increase in stability at high lift coefficients. The ineffectiveness of the flap on the free-flight model was probably caused by the different airfoil section.

The results of further tests made using a stall control vane in an effort to obtain a pitching-moment curve corresponding to that of the higher scale tests of UWAL and Wright Field with nose flaps are also presented in figure 7. These results show that the use of the vane gave a satisfactory pitching-moment curve which agreed very well with that obtained with the nose flap in the higher scale tests.

Presented in figure 8 is the variation of the lateral stability parameters,  $C_{Y\beta}$ ,  $C_{n\beta}$ , and  $C_{l\beta}$  with lift coefficient for the original configuration compared with results from UWAL and Wright Field. The UWAL data have been transferred to 26.7 percent of the mean aerodynamic chord which corresponds to the free-flight-tunnel data while the Wright Field data are presented about 24.2 percent of the mean aerodynamic chord because no lateral-force data were available to use in transferring these data. The results of figure 8 show that the free-flight-tunnel model with tail on had about the same directional stability  $C_{n\beta}$  as the Wright Field model and



somewhat more than the UWAL data indicate. Fairly good agreement is shown in the effective dihedral parameter  $C_{l\beta}$  although the free-flight-tunnel results show lower values throughout the lift range than either the UWAL or Wright Field results. The small effective dihedral was partly caused by the geometric dihedral of  $-4^\circ$  and partly by the large fuselage which force test results of the component parts had shown greatly reduced the positive effective dihedral of the isolated wing.

Presented in figure 9 are the results of tests made to determine the effect on the lateral stability characteristics of the various center vertical tail arrangements used in the flight tests to vary the directional stability.

Figure 10 shows the effect of the stall control vane on the lateral stability characteristics. It may be seen that the vane reduced both the directional stability and effective dihedral over the lift range.

The results of the lateral stability tests are summarized in figure 11 in the form of a stability chart giving the effect of lift coefficient on  $C_{n\beta}$  and  $C_{l\beta}$  with the stall control vane installed and removed.

In figure 12 the increments of directional stability for various tail configurations are presented. These results indicate a large interference effect when the center fin is used in combination with the upper vee tail. For example, at  $C_L = 0$  the large center vertical gave  $\Delta C_{n\beta} = 0.0025$  and the upper vee gave  $\Delta C_{n\beta} = 0.00285$ ; yet with both tails on the total  $\Delta C_{n\beta}$  is only 0.00375 indicating a large loss in tail effectiveness because of mutual interference effects.

Presented in figure 13 are the results of the tests made to determine the aileron effectiveness with the model in the original configuration. These results show that the aileron effectiveness remained nearly constant between  $\alpha = 0^\circ$  and  $12^\circ$  but at  $20^\circ$  the effectiveness is reduced to about half and the yawing moment becomes adverse.

Flight tests. - The results of the flight tests indicated that the longitudinal stability of the model in the original configuration was satisfactory only over the lift coefficient range up to  $C_L = 0.60$ . At higher lift coefficients, the model exhibited a nosing-up tendency associated with the reduction in stability shown in the force tests.

At these lift coefficients it was difficult to steady the model and considerable attention to elevator control was required. At the high lift coefficients the model often stalled and rolled violently off on either wing.

The flights made with the stall control vane on the wings gave no indication of the unstable nosing-up tendency. The longitudinal stability remained nearly the same throughout the lift range and only at lift coefficients above 0.8 was any difficulty in flying the model encountered. Even in these cases there was never a violent stall but only an occasional dropping of a wing which could usually be picked up with the ailerons.

The directional stability and effective dihedral of the model in the original configuration were considered satisfactory over the lift range which could be covered before longitudinal stability difficulties were encountered. There was, however, a slight increase in the tendency to yaw at the higher lift coefficients. The addition of the large center fin improved the flying characteristics slightly by reducing the magnitude of the yawing motion. Removal of the center fin resulted in a small increase in the magnitude of the yawing motion over that of the original configuration but the stability was still considered to be fairly good. At no time during the flights was there any evidence of excessive positive effective dihedral and the lateral oscillations were well damped in all cases.

The behavior of the model was satisfactory for all conditions with ailerons and rudders used together for lateral control or with ailerons used alone although the ailerons became somewhat sluggish at high lift coefficients and there was slightly more yawing with ailerons alone particularly when the center vertical tail was off.

With the stall control vane on, the stability and control characteristics were good throughout the lift range although the aileron control became somewhat sluggish at high lift coefficients as in the original configuration. This result and the data of figure 10 lead to the conclusion that the directional stability of the model in the original configuration would probably be satisfactory over the lift range.

There was no marked effect of lift coefficient on the lateral stability and control characteristics over the lift range tested although slightly more attention to aileron control was required at low lift coefficients because of the small positive effective dihedral.

## CONCLUSIONS

The following conclusions were drawn from the results of the free-flight-tunnel stability and control investigation of an unballasted  $\frac{1}{5}$ -scale model of the McDonnell XP-85 airplane:

1. In the original configuration the model was found to be longitudinally stable up to  $C_L = 0.6$ . At higher lift coefficients there was evidence of a nosing-up tendency which caused the model to stall violently and roll off on either wing.

2. The use of a stall control vane on the wing to simulate the pitching-moment characteristics obtained with the design nose flap in higher scale tests resulted in the model having satisfactory longitudinal stability characteristics over the entire lift range. With the stall control vane there was only a gentle stall; and a dropping wing could usually be picked up by aileron control.

3. The lateral stability and control characteristics were considered to be generally satisfactory for all conditions tested and the rolling and yawing motions were well damped. There was no marked effect of lift coefficient on the lateral stability characteristics over the lift range tested. Slightly more attention to aileron control was required at the lower lift coefficients because of the small positive effective dihedral, and the aileron control was somewhat sluggish near the stall.

Langley Memorial Aeronautical Laboratory  
National Advisory Committee for Aeronautics  
Langley Field, Va.

*John W. Paulson*

John W. Paulson  
Aeronautical Engineer

*Joseph L. Johnson*

Joseph L. Johnson  
Aeronautical Engineer

Approved: *Thomas A. Harris*

for Hartley A. Soule  
Chief of Stability Research Division

REFERENCES

1. Shortal, Joseph A., and Osterhout, Clayton J.: Preliminary Stability and Control Tests in the NACA Free-Flight Tunnel and Correlation with Full-Scale Flight Tests. NACA TN No. 810, 1941.
2. Shortal, Joseph A., and Draper, John W.: Free-Flight Tunnel Investigation of the Effect of the Fuselage Length and the Aspect Ratio and Size of the Vertical Tail on Lateral Stability and Control. NACA ARR No. 3D17, 1943.

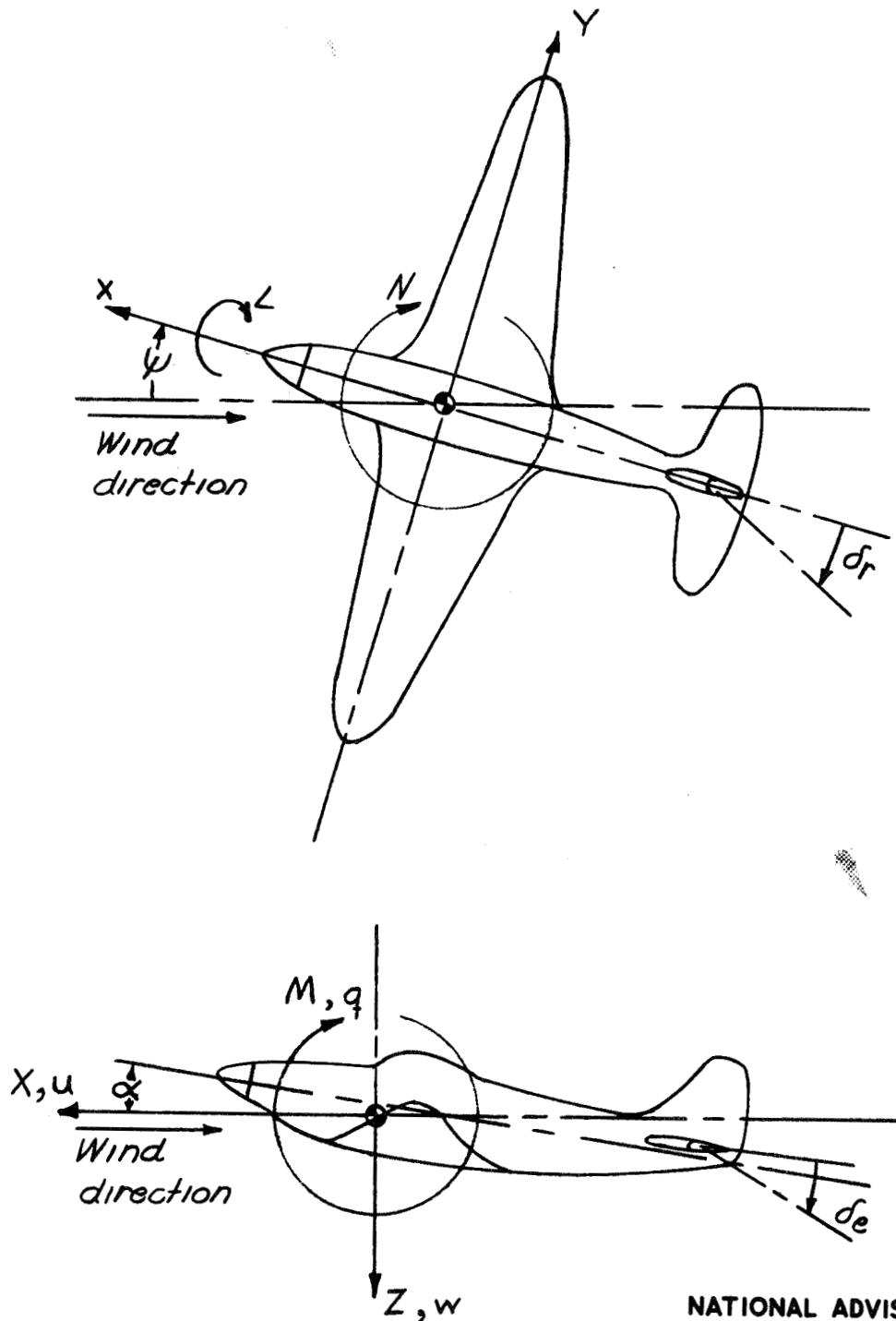
TABLE I.- DIMENSIONAL AND MASS CHARACTERISTICS OF THE MCDONNELL XP-85  
AND SCALED-UP CHARACTERISTICS OF  $\frac{1}{5}$ -SCALE MODEL TESTED  
IN LANGLEY FREE-FLIGHT TUNNEL

	Scaled up	Full scale
Weight, lb . . . . .	1360	4777
Relative density factor $\mu$ , m/p <sub>s</sub> b . . . . .	8.47	29.8
Wing		
Area, sq ft . . . . .	100	100
Span, ft . . . . .	21	21
Aspect ratio . . . . .	4.4	4.4
Sweepback, c/4, deg . . . . .	34	34
Incidence, deg . . . . .	-1	1
Dihedral, deg . . . . .	-4	-4
Taper ratio . . . . .	0.33	0.33
Washout, deg . . . . .	0	5
M.A.C., ft . . . . .	5.16	5.16
Location of M.A.C. behind leading edge root chord, ft . . . . .		
Root chord, ft . . . . .	3.45	3.45
Tip chord, ft . . . . .	7.15	7.15
Distance from nose to L.E. root chord, ft . . . . .	2.38	2.38
Wing loading, W/S, lb/sq ft . . . . .	2.19	1.78
	13.60	47.77
Aileron		
Area, percent wing area, (one) . . . . .	3	3
Span, percent wing span, (one) . . . . .	20	20
Hinge location, percent chord . . . . .	80	80
Nose flap		
Area, percent wing area, (one) . . . . .	2.1	2.1
Span, percent wing span, (one) . . . . .	19.1	19.1
Chord, percent wing chord . . . . .	15	15
Tail		
Vertical fin (upper vee)		
True area, sq ft . . . . .	8.32	8.32
Upper vee (true) sq ft . . . . .	20.40	20.40
(Horizontal projection) sq ft . . . . .	14.40	14.40
Lower vee (true) sq ft . . . . .	11.67	11.67
(Horizontal projection) sq ft . . . . .	8.22	8.22
Design vertical fin, sq ft . . . . .	7.15	7.15
Enlarged vertical fin, sq ft . . . . .	14.10	-----

TABLE I.- DIMENSIONAL AND MASS CHARACTERISTICS  
OF THE MCDONNELL XP-85 AIRPLANE - Concluded

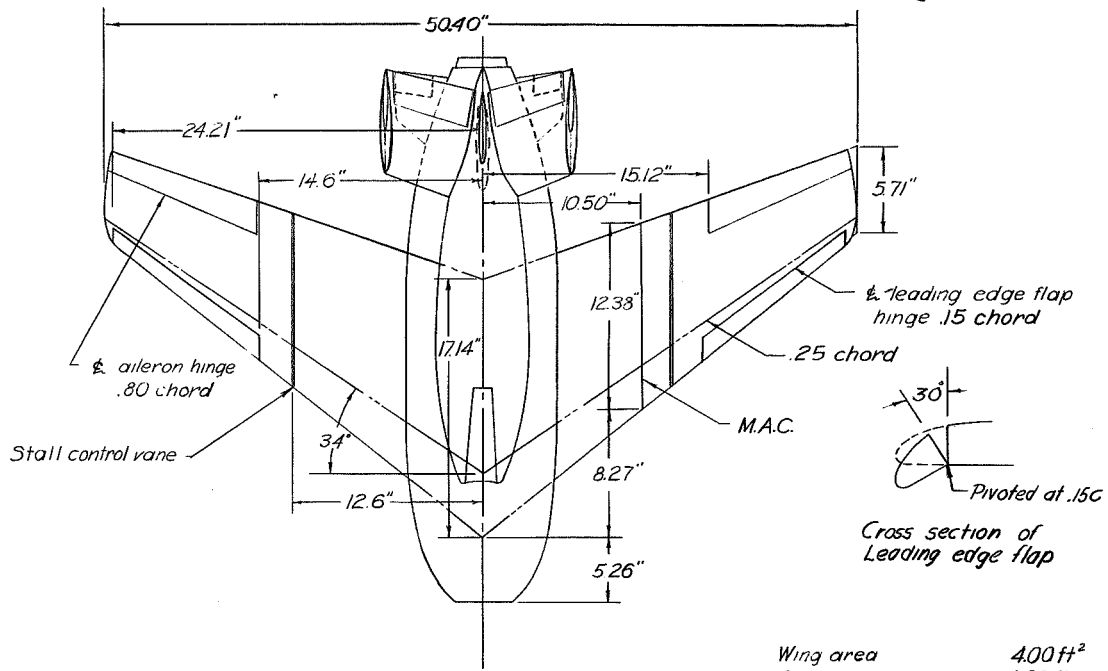
	Scaled up	Full scale
Center-of-gravity location, percent M.A.C. . . . .	26.7(force tests) 22.4(flight tests)	26.7
Distance above thrust line, in . . . . .	0.6	3.1
Percent M.A.C. . . . .	0.01	0.05
Tail length (distance from L.E. root chord wing to c/4 root chord tail)		
Upper tails, ft . . . . .	9.14	9.53
Lower tails, ft . . . . .	9.90	10.30
Moments of inertia		
$I_x$ , slug-ft <sup>2</sup> . . . . .	460	925
$I_z$ , slug-ft <sup>2</sup> . . . . .	1100	1736
$I_y$ , slug-ft <sup>2</sup> . . . . .	850	1485
Radius of gyration to wing span		
$k_x/b$ . . . . .	0.157	0.119
$k_z/b$ . . . . .	0.243	0.163
$k_y/b$ . . . . .	0.213	0.150

NATIONAL ADVISORY  
COMMITTEE FOR AERONAUTICS

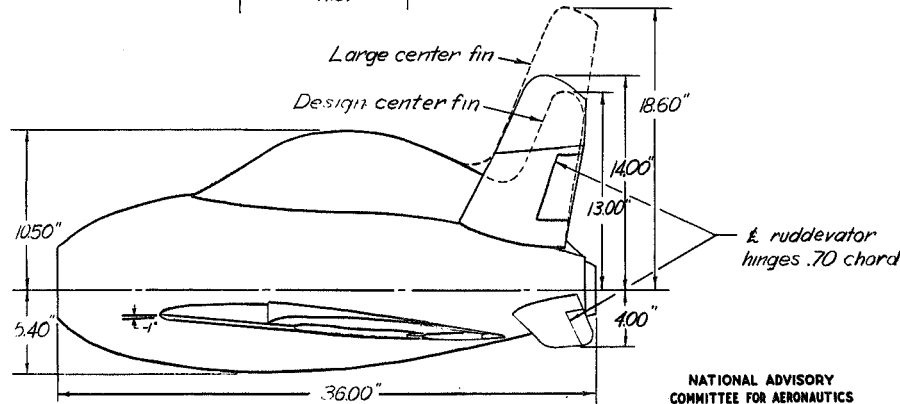
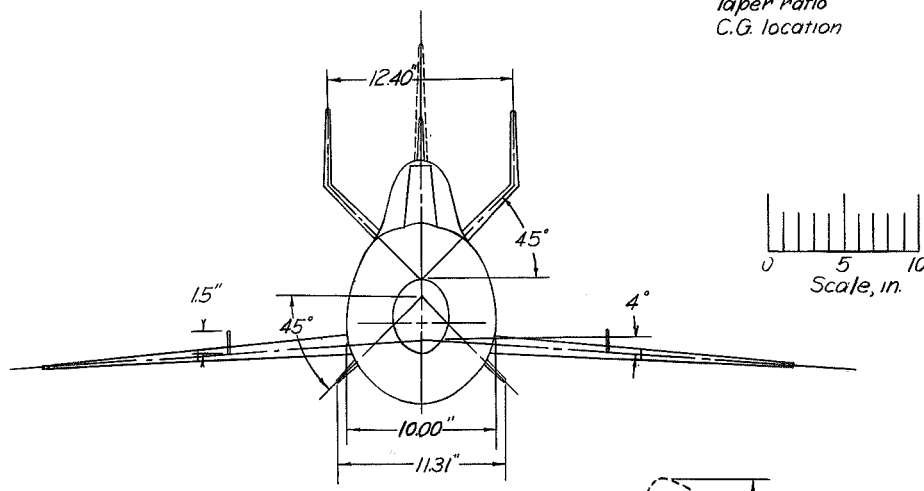


NATIONAL ADVISORY  
COMMITTEE FOR AERONAUTICS

Figure 1. - System of stability axes. Arrows indicate positive directions of moments, forces, control-surface deflections, and linear and angular velocities.



Wing area	4.00 ft <sup>2</sup>
Span	4.20 ft
Aspect ratio	4.40
Taper ratio	.33
C.G. location	.267 M.A.C.



NATIONAL ADVISORY COMMITTEE FOR AERONAUTICS

Figure 2- Three view drawing of the 1/8 scale model of the McDonnell XP-85 tested in the Langley free flight tunnel.



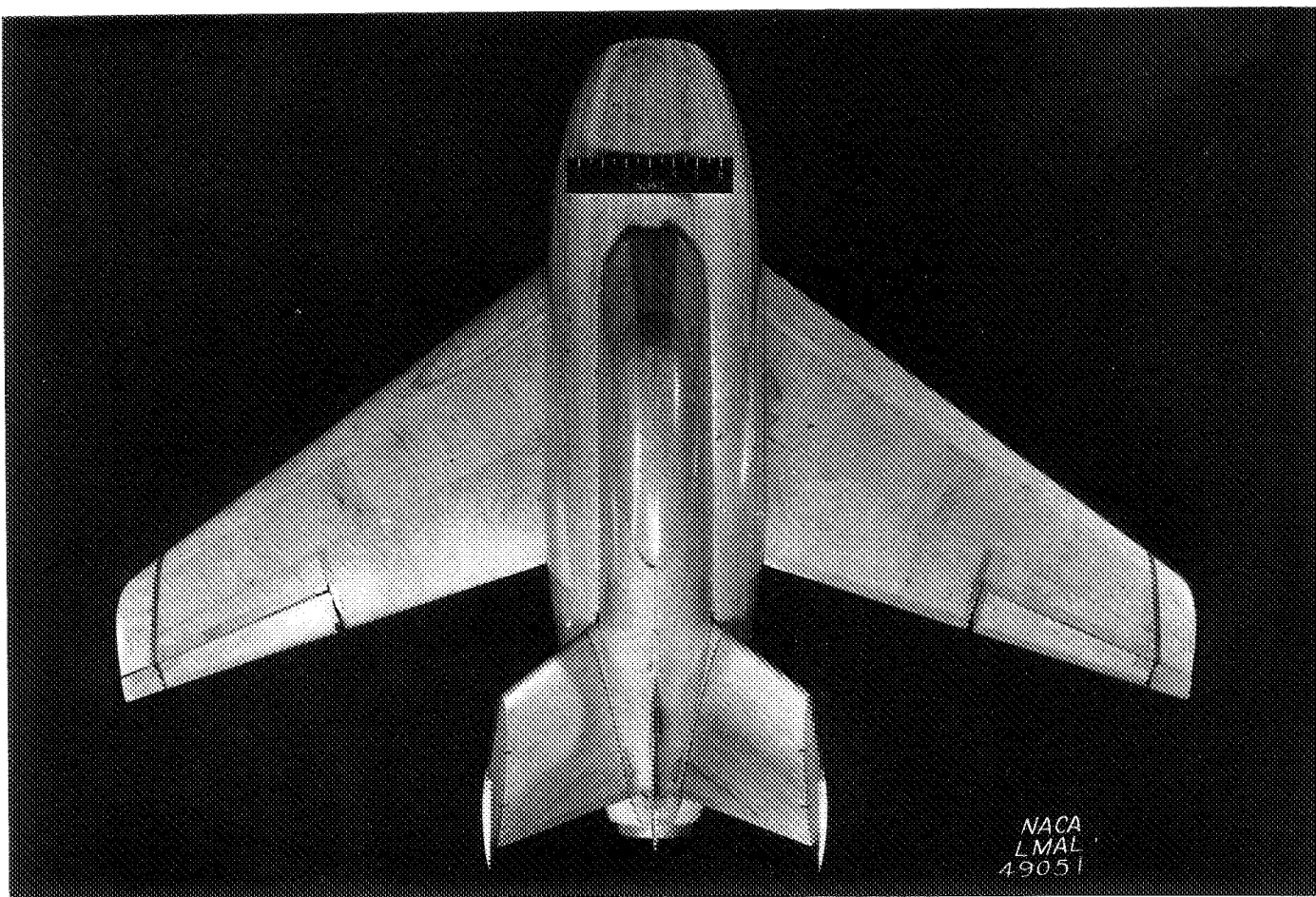


Figure 3.- Top view of  $\frac{1}{5}$ -scale model of the McDonnell XP-85 airplane tested in the Langley free-flight tunnel.

150

NACA RM No. L7C27

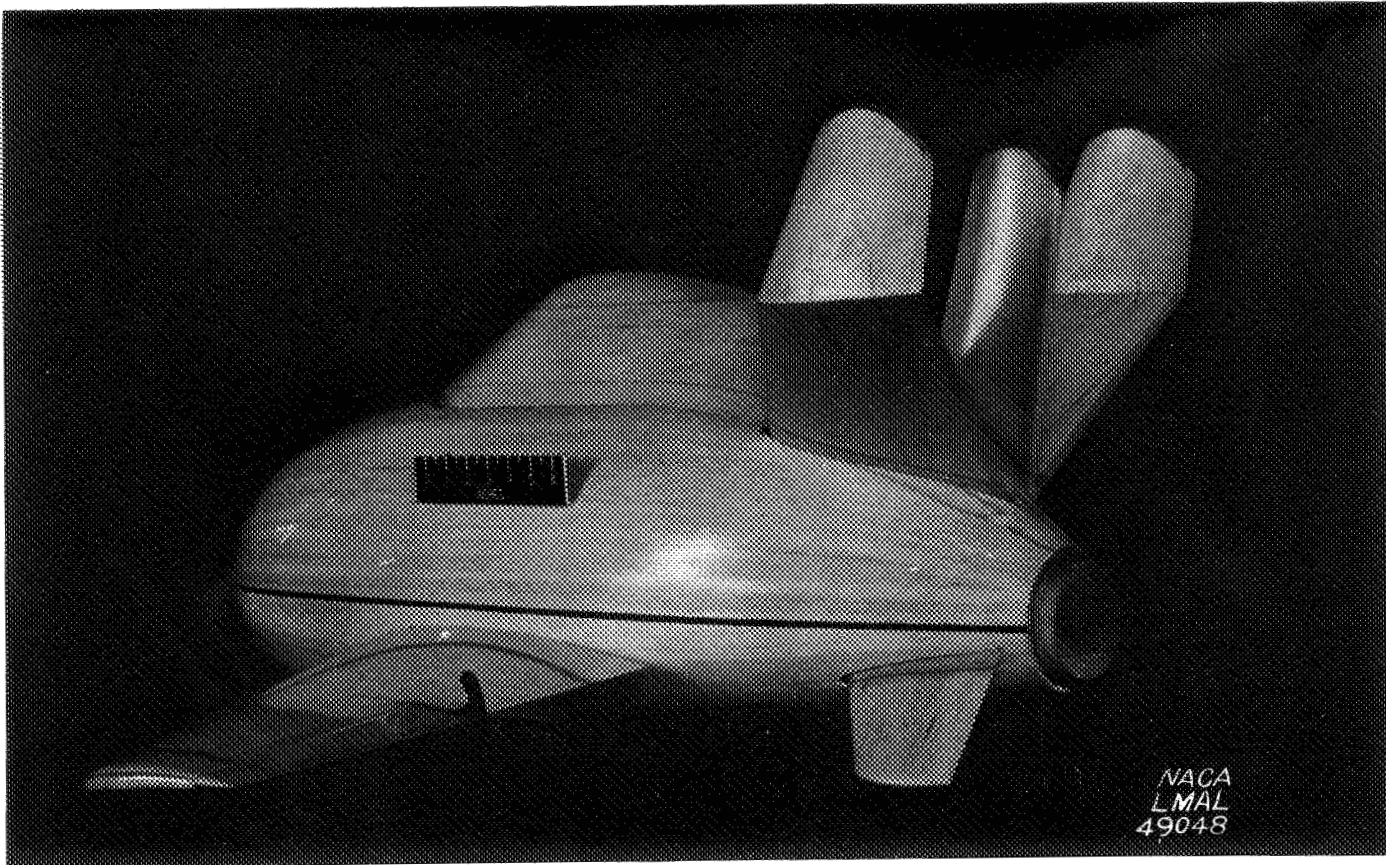


Figure 4.- Three-quarter rear view of  $\frac{1}{5}$ -scale model of the McDonnell XP-85 airplane with design center fin tested in the Langley free-flight tunnel.

NATIONAL ADVISORY COMMITTEE FOR AERONAUTICS  
LANGLEY MEMORIAL AERONAUTICAL LABORATORY - LANGLEY FIELD VA

Fig. 4

1  
2  
3  
4  
5  
6  
7  
8  
9  
10  
11  
12  
13  
14  
15  
16  
17  
18  
19  
20  
21  
22  
23  
24  
25  
26  
27  
28  
29  
30  
31  
32  
33  
34  
35  
36  
37  
38  
39  
40  
41  
42  
43  
44  
45  
46  
47  
48  
49  
50

NACA RM No. L7C27

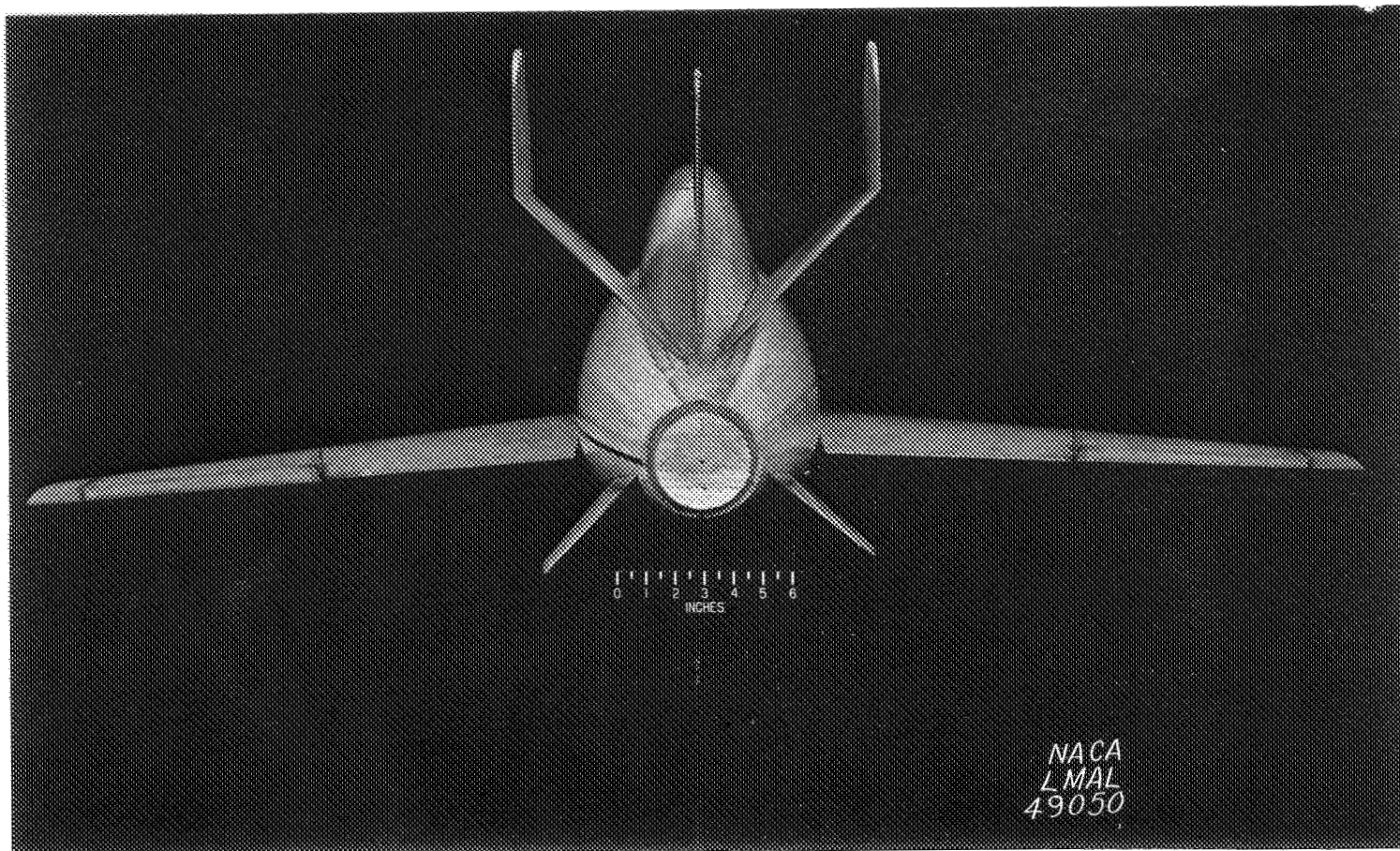


Figure 5.- Rear view of  $\frac{1}{5}$ -scale model of the McDonnell XP-85 airplane with design center fin tested in the Langley free-flight tunnel.

NATIONAL ADVISORY COMMITTEE FOR AERONAUTICS  
LANGLEY MEMORIAL AERONAUTICAL LABORATORY - LANGLEY FIELD, VA.

Fig. 5

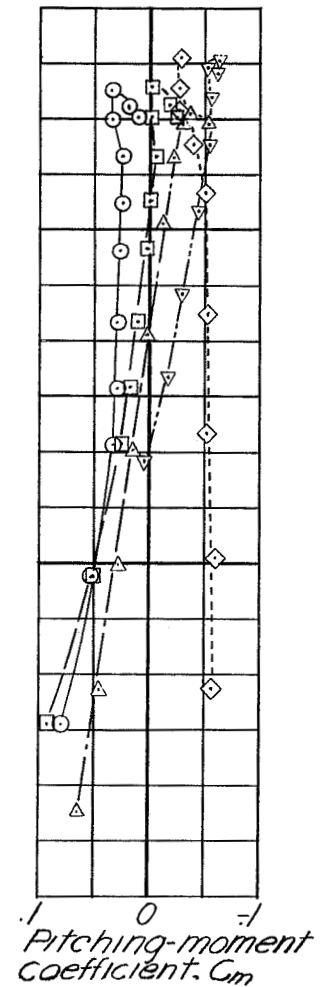
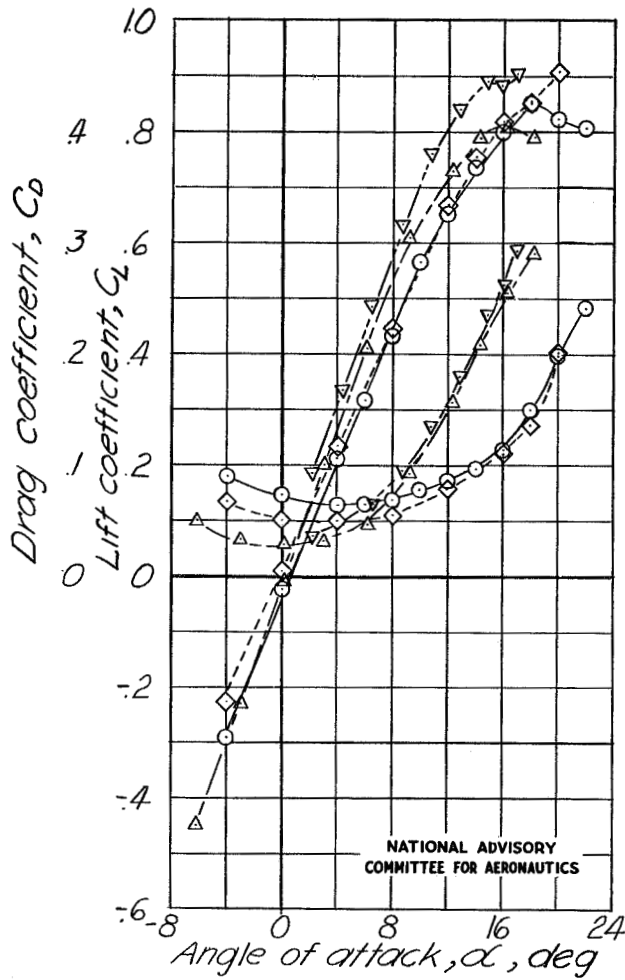
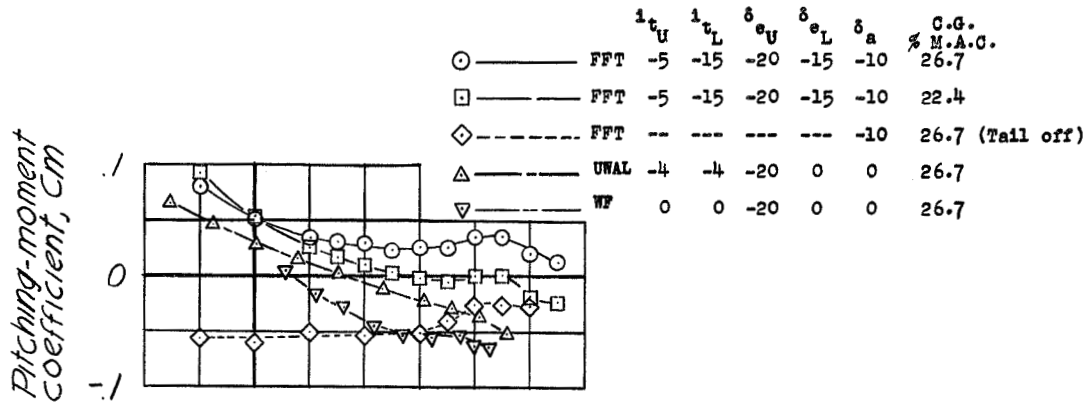


Figure 6.-Lift, drag, and pitching-moment characteristics of the 1/5-scale model of the Mc Donnell XP-85 airplane tested in the Langley free-flight tunnel compared with similar unpublished data from UWAL and Wright Field. Original Configuration  $\psi = 0$ .  $S_r = 0$ .

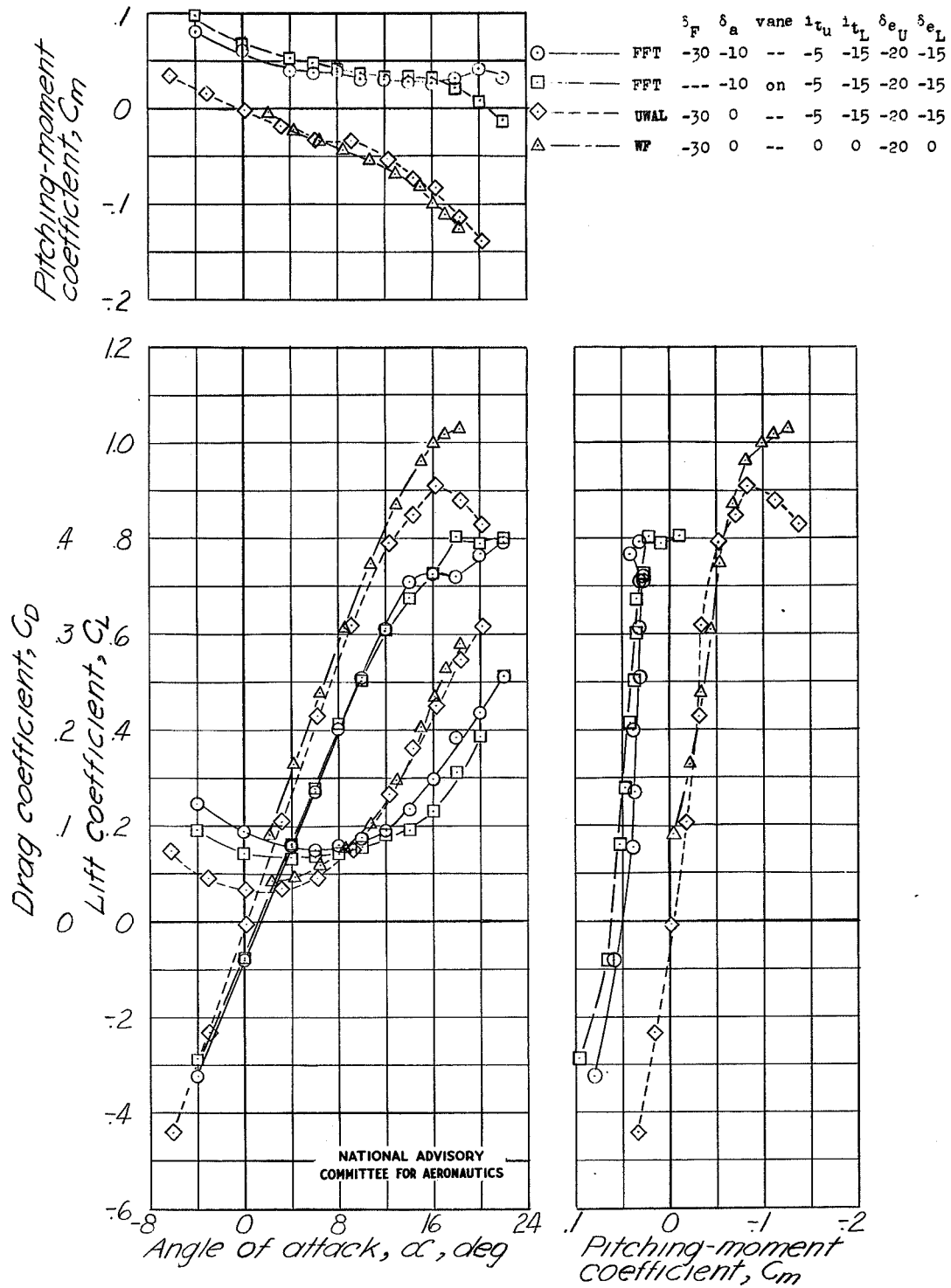


Figure 7.-Lift, drag, and pitching-moment characteristics of the 1/5-scale model of the McDonnell XP-85 airplane with design nose flap and with stall control vane tested in the Langley free-flight tunnel compared with unpublished nose flap data from UWAL and Wright Field.  $\psi=0^\circ$ ; C.G. = 26.7 percent MAC.,  $\delta_r=0^\circ$ .

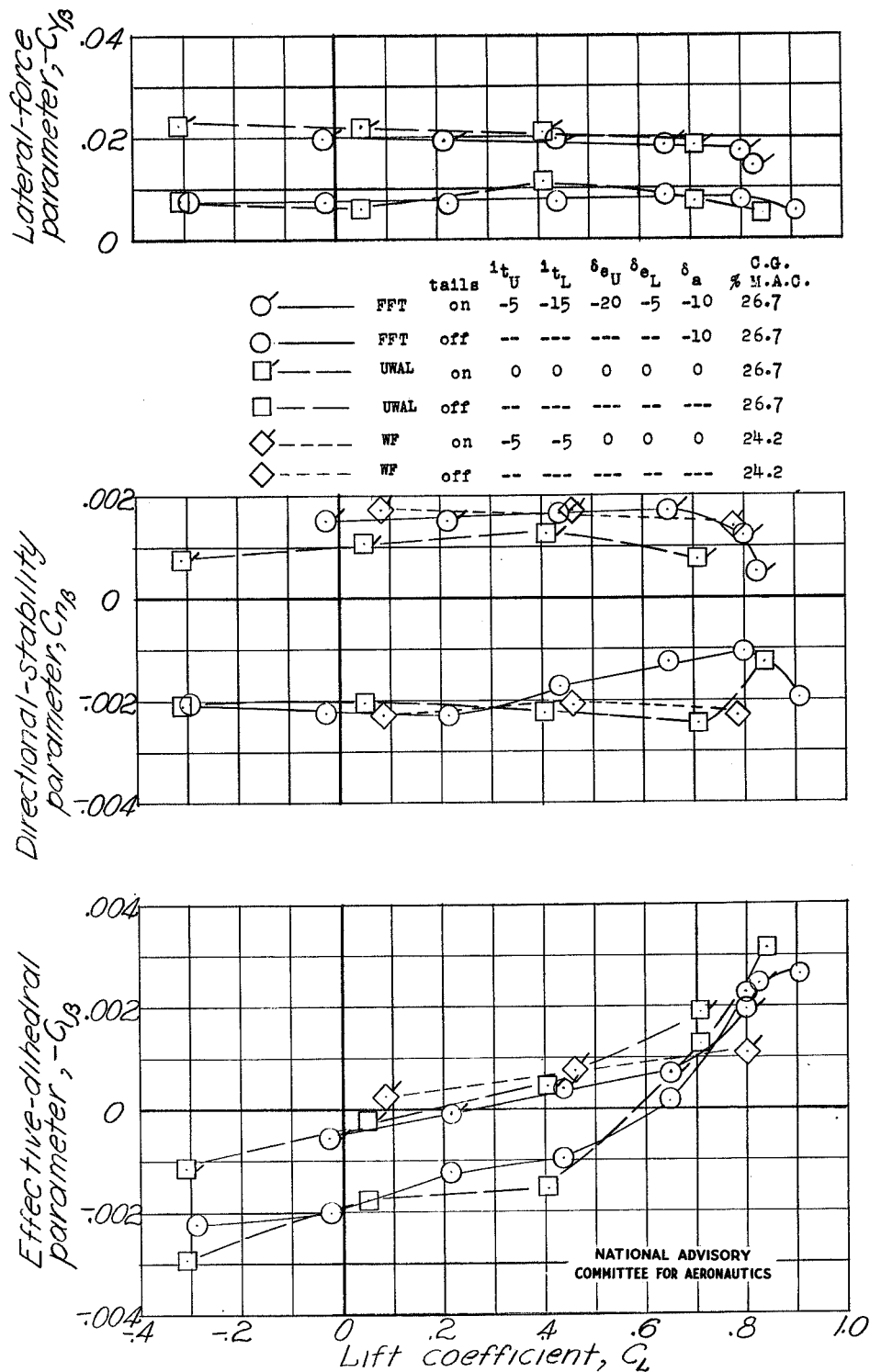


Figure 8.-Lateral stability characteristics of the  $1/8$ -scale model of the McDonnell XP-85 airplane tested in the Langley free flight tunnel compared with the unpublished data from UWAL and Wright Field. Original configuration  $\delta_r = 0^\circ$ .

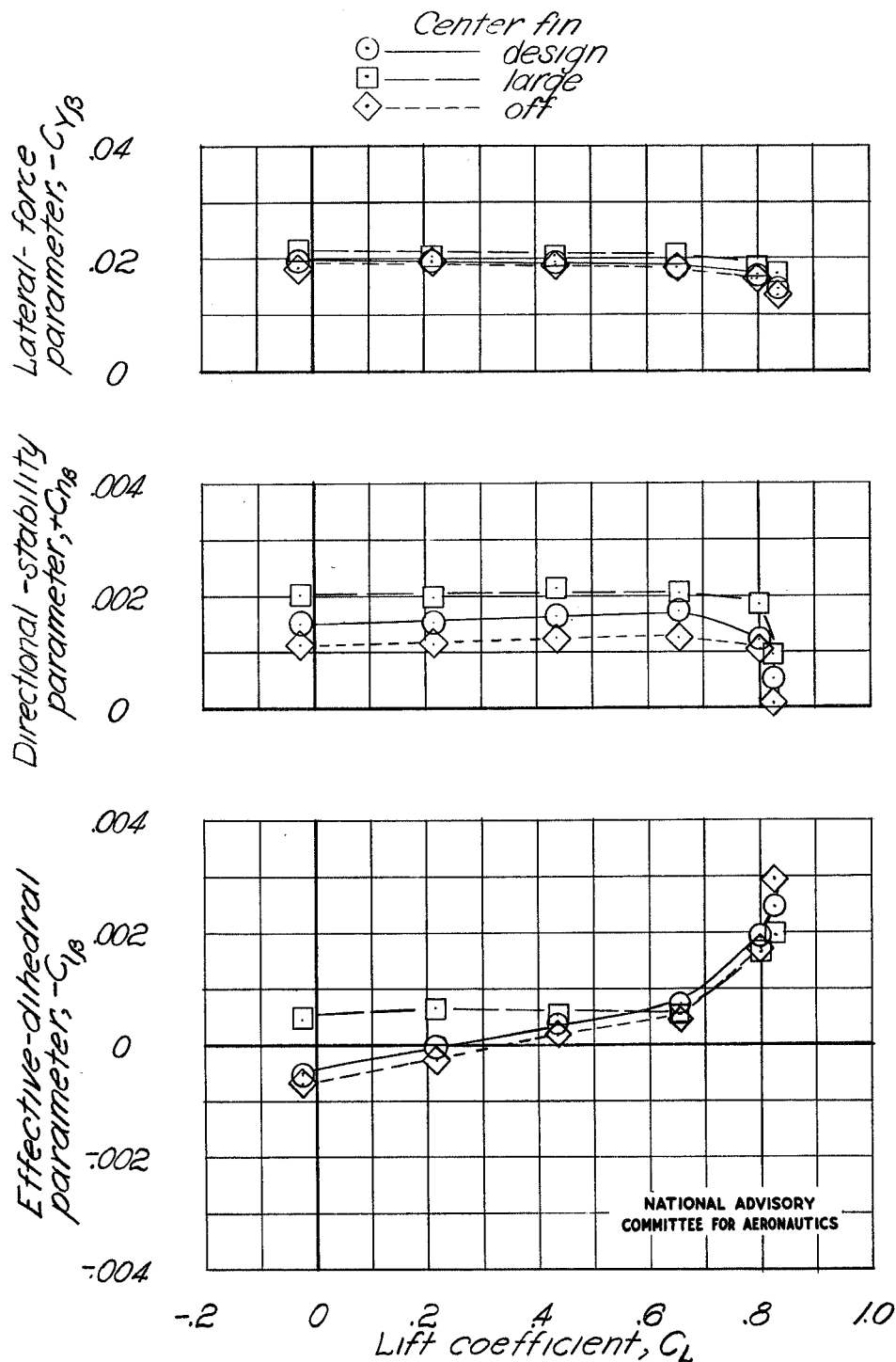


Figure 9.-Effect of vertical tail configuration on lateral stability characteristics of the 1/5-scale model of the Mc Donnell XP-85 airplane tested in the Langley free flight tunnel. C.G.=26.7 percent M.A.C.,  $q=3.0$ ,  $\delta a=-10^\circ$ ,  $\delta r=0$ ,  $\delta e_u=-20^\circ$ ,  $\delta e_L=-15^\circ$ ,  $l_u=-5^\circ$ ,  $l_L=-15^\circ$ .

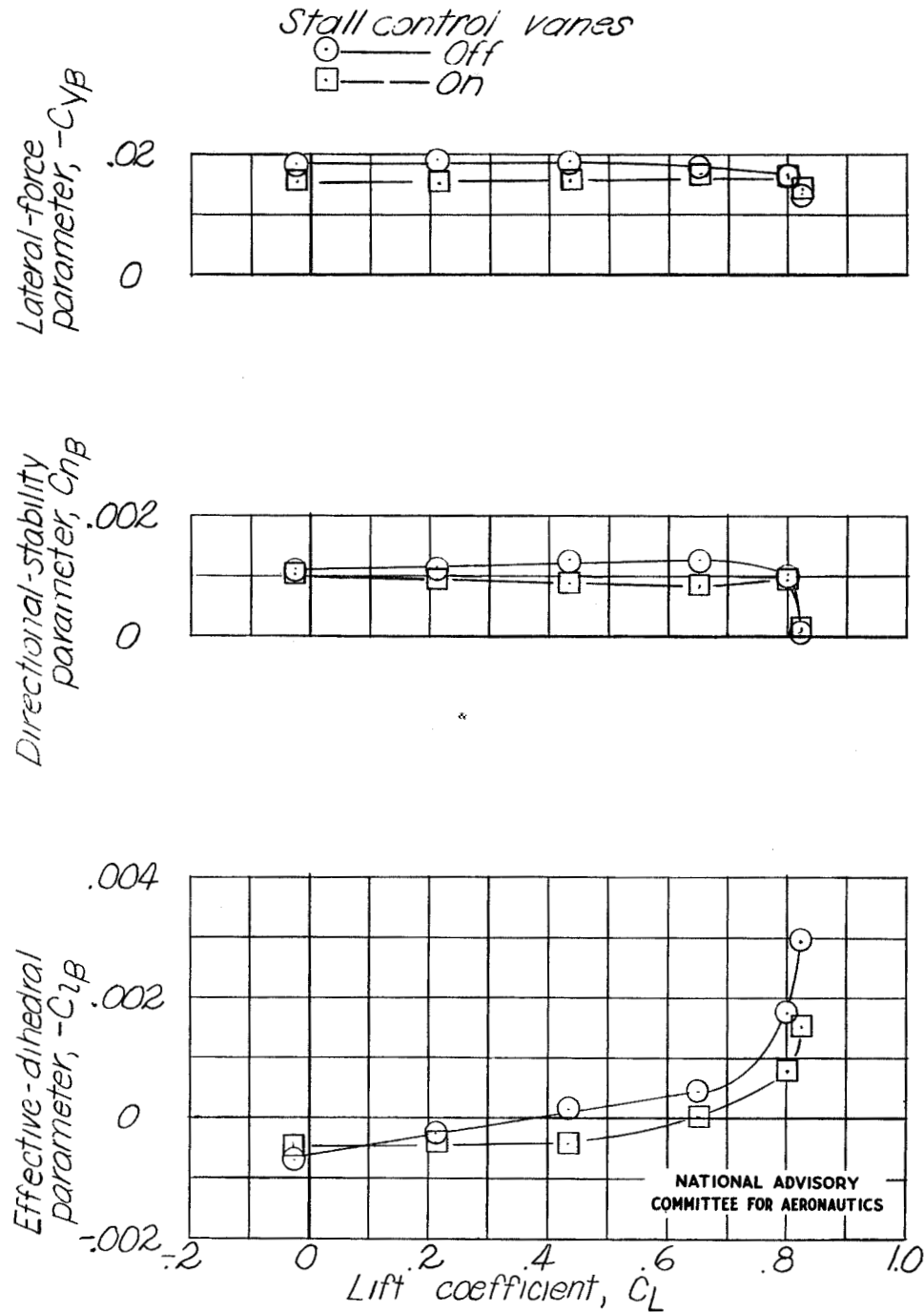


Figure 10.—Effect of stall control vanes on the lateral stability characteristics of the Mc Donnell XP-85 airplane tested in the Langley free flight tunnel. C.G. = 26.7 percent M.A.C.,  $q = 3.0$ ,  $\delta a = -10^\circ$ ,  $\delta e_u = -20^\circ$ ,  $\delta e_L = -15^\circ$ ,  $l_{u_0} = -5^\circ$ ,  $l_{L_2} = -15^\circ$ . Center fin off.



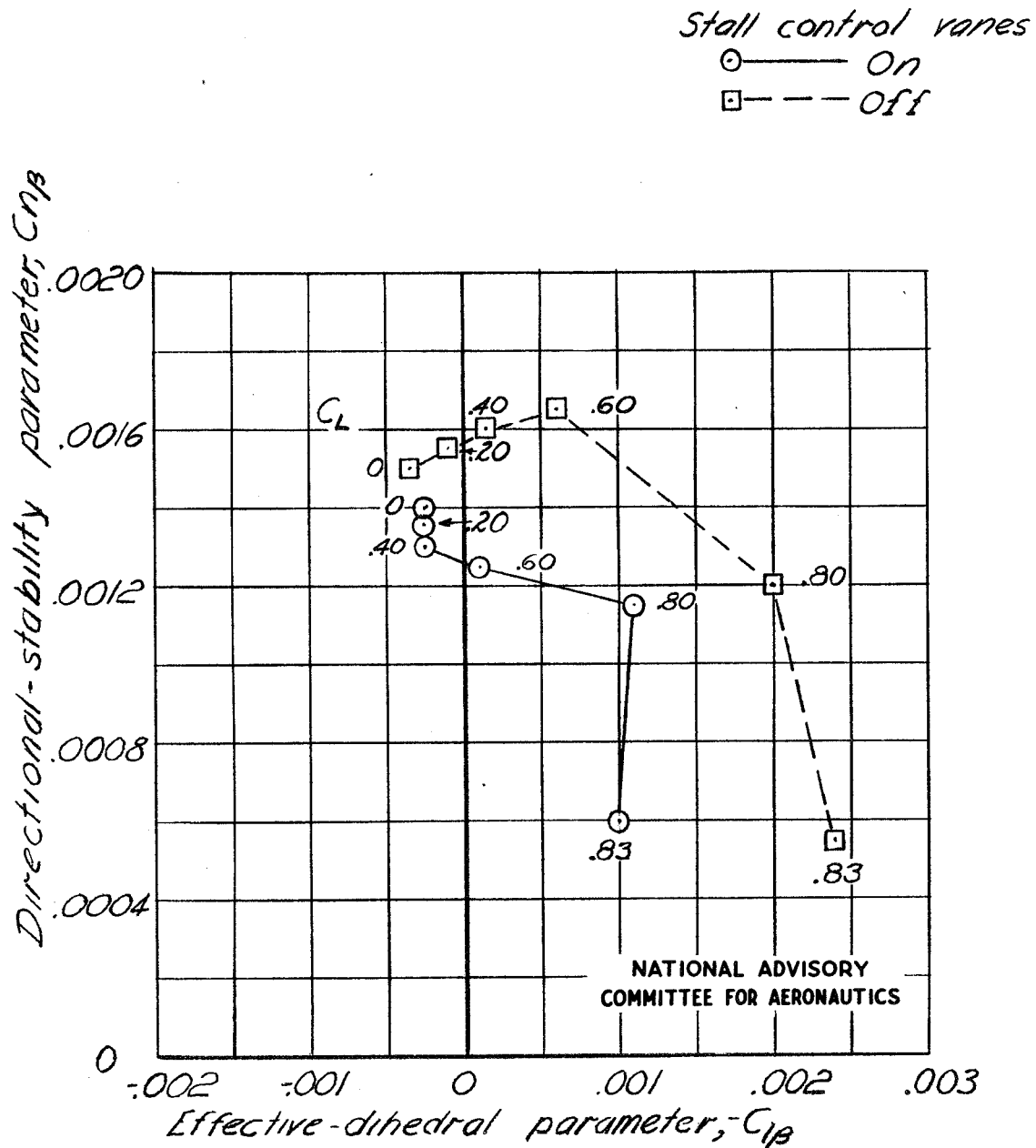


Figure 11.- Variation of lateral stability parameters  $C_{n\beta}$  and  $C_{I\beta}$  with lift coefficient for the 1/5-scale model of the McDonnell XP-85 airplane tested in the Langley free-flight tunnel. C.G. = 26.7 percent M.A.C.,  $q = 3.0$ ,  $\delta_a = -10^\circ$ ,  $\delta_{e_U} = -20^\circ$ ,  $\delta_{e_L} = -15^\circ$ ,  $i_{t_U} = -5^\circ$ ,  $i_{t_L} = -15^\circ$ . Design vertical tail.

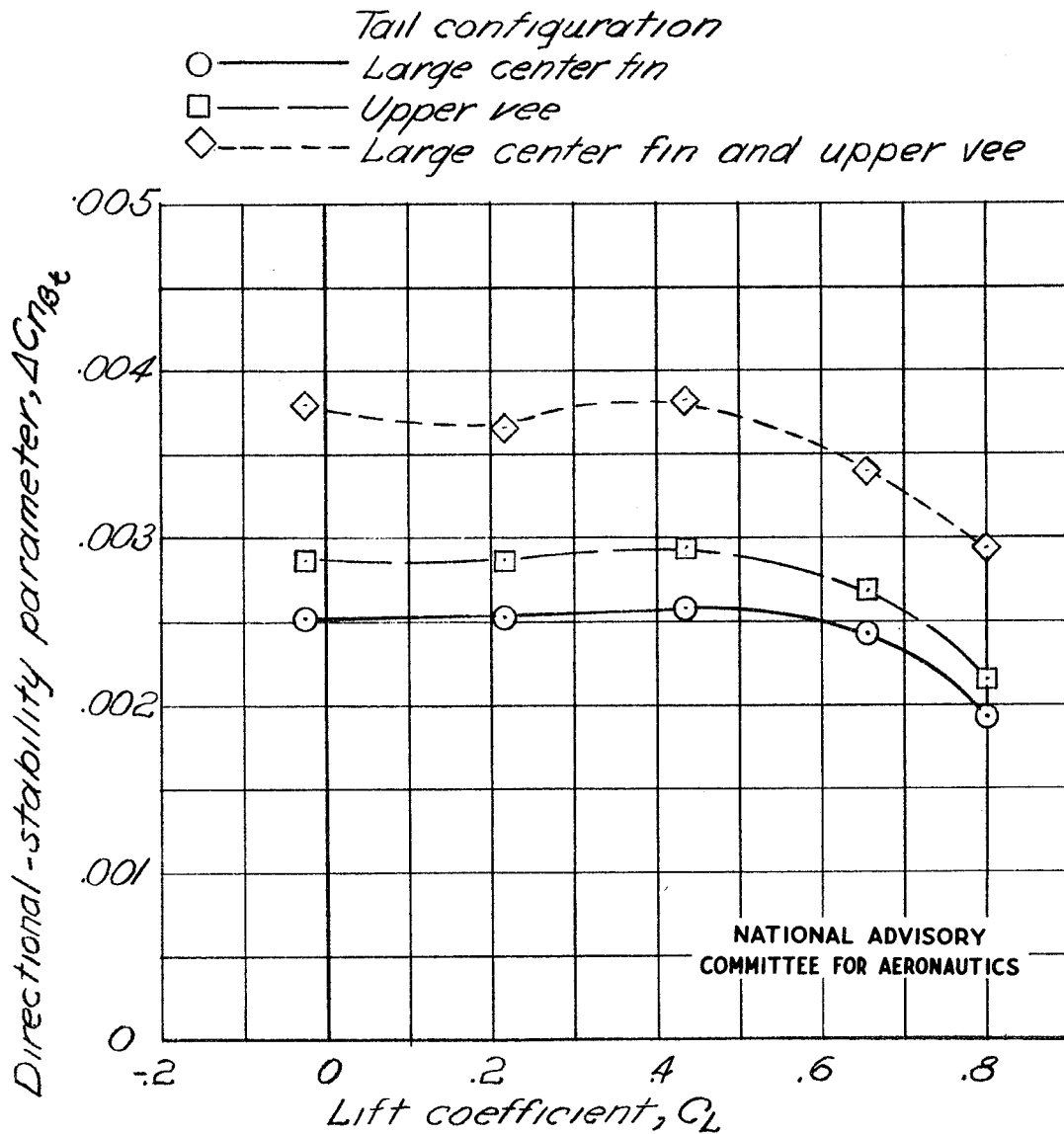


Figure 12.- Effect of tail components on the directional stability parameter  $\Delta C_{n\beta}$ , as determined from force tests of the  $\frac{1}{5}$ -scale model of the McDonnell XP-85 in the Langley free flight tunnel. C.G. = 26.7 percent M.A.C.,  $q = 3.0$ ;  $\delta\alpha = -10^\circ$ ;  $\delta r = 0^\circ$ ;  $\delta e_U = -20^\circ$ ;  $\delta e_L = -15^\circ$ ;  $\delta u = -5^\circ$ ;  $\delta w = -15^\circ$ .

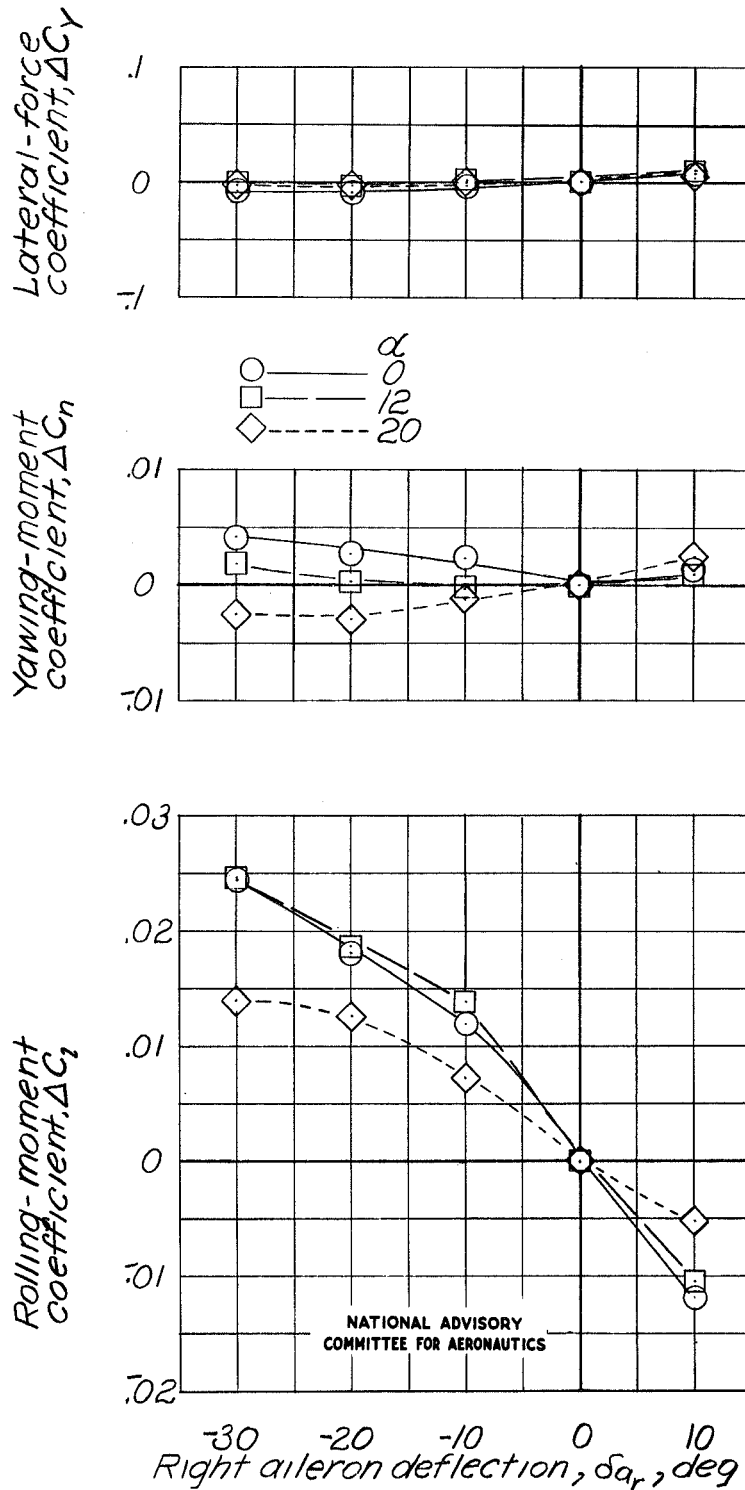


Figure 13.-Variation of aileron effectiveness with angle of attack for the 1/5-scale model of the Mc Donnell XP385 airplane tested in the Langley free flight tunnel. C.G. = 26.7 percent M.A.C.,  $q = 3.0$ ,  $\delta_e = 0^\circ$ ,  $\delta_r = 0^\circ$ ,  $\delta_{aL} = -10^\circ$ ,  $l_{u_1} = -5^\circ$ ,  $l_{u_2} = -15^\circ$ . Normal vertical tail.

NASA Technical Library



3 1176 01437 5068